Control of Different Reactive Distillation Configurations

Shih-Bo Hung and Ming-Jer Lee
Dept. of Chemical Engineering, National Taiwan University of Science and Technology, Taipei 106-07, Taiwan

Yeong-Tarng Tang, Yi-Wei Chen, I-Kuan Lai, Wan-Jen Hung, Hsiao-Ping Huang, and Cheng-Ching Yu
Dept. of Chemical Engineering, National Taiwan University, Taipei 106-17, Taiwan

DOI 10.1002/aic.10743
Published online December 15, 2005 in Wiley InterScience (www.interscience.wiley.com).

Three different flowsheets have been proposed for acetic acid esterification of acetic acid with alcohols ranging from C1 to C5 according to the ranking of normal boiling points and immiscibility. This work explores the similarities and differences in the dynamics and control of these three types of flowsheets. The degree of process nonlinearity is analyzed qualitatively based on the residue curve map and the boiling point ranking and it can be computed quantitatively based on the fraction of "sign reversal" for all tray temperatures or based on Allgower's nonlinearity measure. These measures provide useful information to the potential problems in closed-loop control. Next, a systematic design procedure is proposed to devise control structures for all three types of flowsheets for these five esterification systems. The simulation results reveal that reasonable control can be achieved for all five systems with different degrees of asymmetry in closed-loop responses as predicted by the nonlinearity measures. Dual-temperature control and one-temperature/one-composition control are studied. Simulation results clearly show that the simple decentralized control provides a workable solution for highly nonlinear reactive distillation columns under various flowsheet configurations. © 2005 American Institute of Chemical Engineers *AIChE J,* 52: 1423–1440, 2006
Keywords: reactive distillation, esterification, process control, temperature control, composition control, nonlinearity

Introduction

Reactive distillation combines reaction and separation in a single unit that provides substantial economic incentives for some chemical processes. The literature and patents in reactive distillation have grown rapidly in recent years as surveyed by Malone and Doherty.[1] The books by Doherty and Malone[2] and Sundmacher and Kienle[3] give updated summaries in the field. The review article of Taylor and Krishna[4] describes potential advantages, modeling, simulation, and hardware configurations of reactive distillation. However, the multifunctional nature of the reactive distillation complicates already very nonlinear dynamics of either reactors or separators. Thus, the dynamics and control of reactive distillation are less obvious compared to those of its single-unit counterparts.

The last decade has seen a steady growth in the number of articles that deal with control of reactive distillation column, from a mere handful to over a dozen. Roat et al.,[5] among the first, propose a two-temperature control structure for an industrial column in which two fresh feeds are manipulated by two tray temperatures. This is a rather "unconventional" control structure with respect to the distillation control.[6] The reaction considered is the methyl acetate production with a reversible reaction with two reactants and two products (that is, A + B ↔

Correspondence concerning this article should be addressed to C.-C. Yu at ccyu@ntu.edu.tw.

C + D). Moreover, the esterification is carried out in a "neat"—that is, no excess reactant—flowsheet as opposed to an "excess-reactant" flowsheet, as defined by Luyben and coworkers.[7-11] The "excess-reactant" flowsheet requires two columns to achieve high purity product and is thus more expensive. The "neat" flowsheet has a greater economical potential because only one column is needed. However, it is more difficult to control because two reactants must be fed in the "exact" amount to satisfy the stoichiometry down to the last molecule.[8-11]

Luyben is among the first to recognize this fact and, therefore, not so conventional control structures results. Luyben and coworkers propose eight control structures for the "neat" reactive distillation (CS1–CS6 in Al-Arfaj and Luyben[7]; CS6–CS7 in Al-Arfaj and Luyben[8]; CS7–CS8 in Kaymak and Luyben[9,10]). Typically, a generic distillation column with a second-order reversible reaction is investigated. In addition to the control of continuous reactive distillation for A + B ↔ C + D systems, control of reactive distillations for fuel ether (MTBE, ETBE, TAME) has been studied by Sneesby et al.,[11] which corresponds to a reactive kinetics of two reactants and one product, that is, A + B ↔ C. Linear and nonlinear control of semibatch reactive distillation for ethyl acetate production has been explored by Engell and Fernholz.[12] Nonlinear estimation and control of a two-stage reaction has been studied by Grüner et al.[13] Because of the difference in the mode of operation (batch vs. continuous) and in the reaction kinetics (A + B ↔ C + D vs. A + B ↔ C), the potential problems of the "neat" flowsheet have not been emphasized.

This work continues the earlier effort to explore the control of acetic acid esterification with different alcohols (ranging from C1 to C5[14]). The esterifications lead to three different types of flowsheets (categories I–III) with different economical potentials.[15] The esterification processes explored share a common characteristic—"neat" flowsheet—while maintaining their own process configurations and the object of this work is to devise control structures for these three different categories of reactive distillation. A systematic procedure is proposed for the control structure design that is applicable to all three process configurations. Temperature as well as composition controls are explored and interaction between design and control is discussed.

Process Characteristics

Process studies

As indicated by Tang et al.,[14] the esterification of acetic acid with different types of alcohols (ranging from C1 to C5) can be classified into three flowsheets, type I, type II, and type III, as shown in Figure 1. The gradual change in the process configuration is the direct consequences of: (1) increased immiscibility (Figure 2) and (2) the shift of the ranking of the two products (water and acetate). Table 1 gives the optimized design for the production of methyl acetate (MeAc; type I), ethyl acetate (EtAc; type II), isopropyl acetate (IPAc; type II), butyl acetate (BuAc; type III), and amyl acetate (AmAc; type III) systems.

Steady-state analysis indicates that the type I and type III systems are more economical than the type II system.[14] Here we set out to explore the dynamic controllability of these three flowsheets. Importantly, we sought to devise a systematic approach to the control of these three types of reactive distillations. In this work, all the results are obtained from steady-state and dynamic simulations using Aspen Plus and Aspen Dynamics.

Qualitative analysis

The residual curve map (RCM) offers useful insights to the operation of the reactive distillation systems. Let us use the EtAc system to illustrate the separation behavior in the reactive distillation (Figures 1 and 2). The top product composition of the reactive distillation tends to converge toward the unstable "node" of the ternary minimum boiling azeotrope as indicated as an open circle in Figure 2. After withdrawing relatively pure water from the aqueous phase of the decanter, the organic phase is fed to a stripper to obtain high purity EtAc (Figure 1B). The separation performed in the stripper is confined by a distillation boundary that is defined by two binary and one ternary azeotropes as shown in the top left corner of Figure 2. Again, the product EtAc is a stable "node" that can be obtained in a straightforward manner, if sufficiently large separation capability is provided. In summary, from process configuration and the RCM, it is clear that both products (water and EtAc) of the ethanol esterification are "nodes." A similar argument can be applied to the IPAc system as shown in Figures 1 and 2.

Type III reactive distillation is also analyzed here. The BuAc system is used to illustrate the product formation. First, the overhead product converges toward the ternary azeotrope as can be seen in Figure 2. Consequently, the top product, water, is withdrawn from the aqueous phase of the decanter (Figure 1). Because the BuAc is the heaviest component, it is again a stable node. Thus, both top and bottom products can be obtained by providing sufficiently large separation capacity to the stripping and rectifying sections.

The type I reactive distillation for MeAc production, on the other hand, shows a different process characteristic. If the acetic acid is totally consumed toward the bottoms, we can obtain high-purity water; however, in general, the bottoms product is a saddle as shown in Figure 2. Toward to the overhead, the methyl acetate corner is, again, a saddle because of two minimum boiling binary azeotropes. It thus becomes clear that difficulty in the control and operation of the MeAc system is expected. Importantly, the RCMs (Figure 2) and the process configurations (Figure 1) provide useful information to potential operation problems of reactive distillation systems.

Quantitative analysis

Manipulated Inputs. Before getting into detailed quantitative analysis, we need to identify manipulated variables for these three different types of processes. As pointed out by Luyben,[15] it is important to maintain the stoichiometric balance for the "neat" reactive distillation. Al-Arfaj and Luyben[8] choose to use one of the feed rates and, here, the feed ratio (*FR*) is used as the manipulated variable. In addition to maintaining the stoichiometric balance, in theory, we need to control two product compositions using two manipulated variables. However, for reactions such as A + B ↔ C + D, if the conversion is properly maintained and the product flow rates are equally distributed, one-end composition control will do a fairly good job. For a type I flowsheet of MeAc production, following

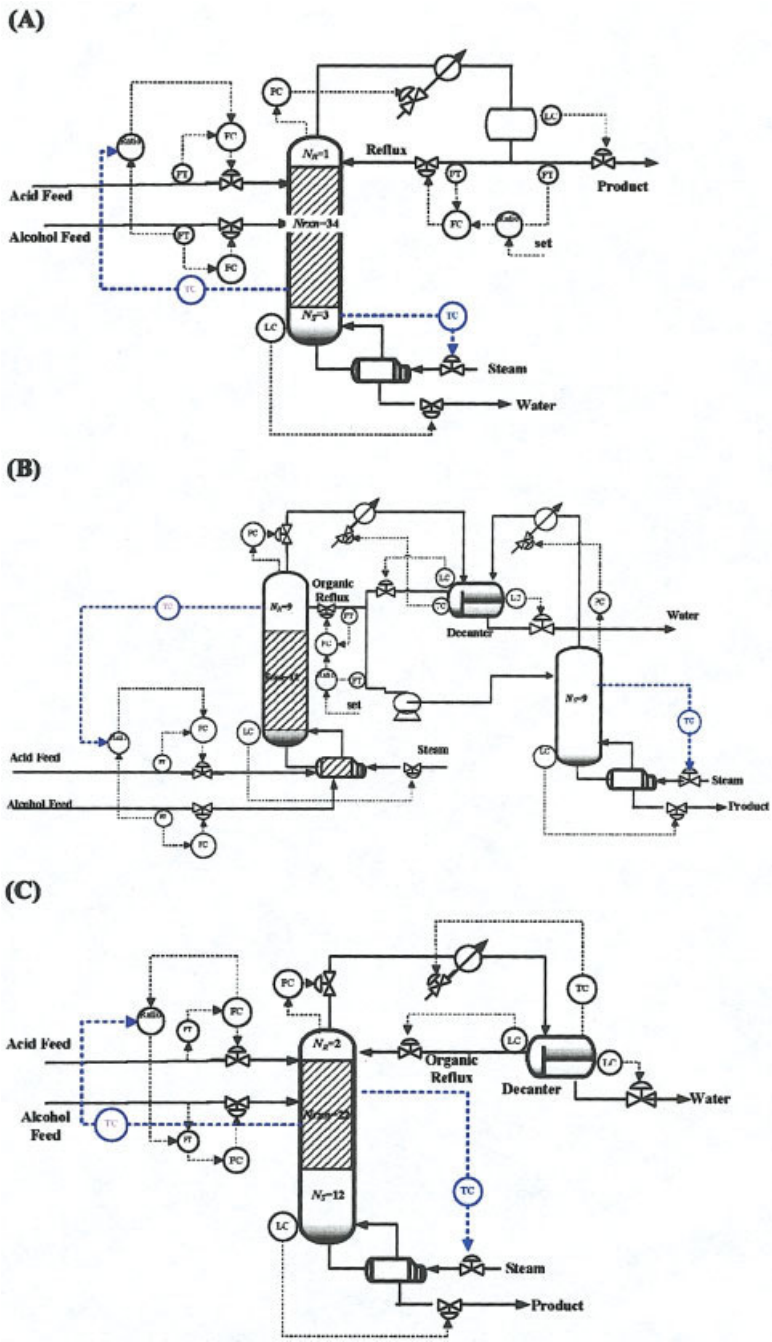

Figure 1. Process flowsheets for temperature control configurations for type I (A), II (B), and III (C) systems.

[Color figure can be viewed in the online issue, which is available at www.interscience.wiley.com.]

Al-Arfaj and Luyben,[8] we choose to control the bottoms composition using vapor boilup while fixing the reflux ratio. For a type II flowsheet, the product composition of water from the first column (RD column) is determined by liquid–liquid equilibrium, so no composition control is necessary. However, the reflux ratio of the RD column is fixed. The acetate production is withdrawn from the stripper and the composition is controlled by manipulating the vapor boilup as shown in Figure 1. Similar to the type II flowsheet, a decanter is used for type III flowsheets to separate the water from the column overhead and, therefore, composition control is not necessary and the origin phase is totally refluxed back to the column. This is similar to the configuration studied by Huang et al.[16] and Chiang et al.[17] The bottoms acetate composition, however, is controlled by changing the reboiler duty. Note that all the control structures mentioned in this section are under temperature control. In summary, the manipulated variables are:

- Type I: feed ratio, and reboiler duty (fixing reflux ratio)
- Type II: feed ratio and reboiler duty in the stripper (fixed organic reflux ratio in RD)
- Type III: feed ratio and reboiler duty (organic phase totally refluxed)

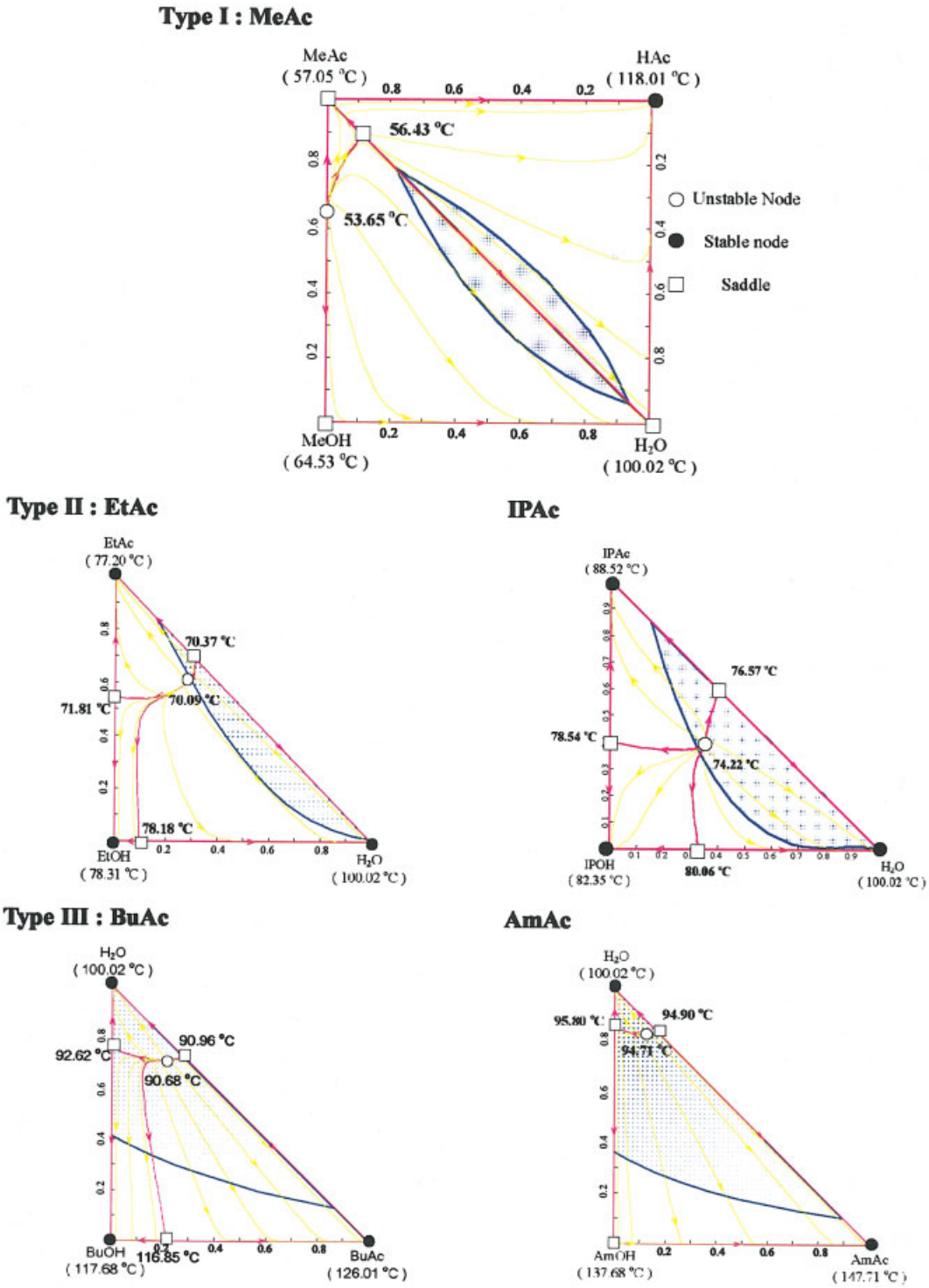

Figure 2. Residual curve maps and two-liquid zone for five esterification systems.

[Color figure can be viewed in the online issue, which is available at www.interscience.wiley.com.]

Nonlinearity and Output Multiplicity. Once the manipulated variables have been determined, we then seek to evaluate process nonlinearity for these three different types of flowsheets. The tray temperatures are treated as the state variables. The manipulated variables are the heat input Q_R and feed ratio *FR*, respectively. First, the upper and lower bounds of the steady-state gains between the tray temperatures and the manipulated variables (Q_R and *FR*) are obtained for a range of input variations. In this work, -5 to $+5\%$ changes in the Q_R and -1 to $+1\%$ changes in the *FR* are made. Note that, for a truly linear system, the upper and lower bounds should coincide with each other. Figure 3 clearly shows that the reactive

Table 1. Steady-State Operating Condition and Total Annual Cost (TAC) for Reactive Distillation Designs of Five Esterification Systems

	System						
	(i) MeAc	(ii) EtAc		(iii) IPAc		(iv) BuAc	(v) AmAc
Column Configuration	RD	RD	Stripper	RD	Stripper	RD	RD
Total no. of trays including the reboiler	39	20	10	26	8	34	37
No. of trays in stripping section (N_S)	3		9		7	9	12
No. of trays in reactive section (N_{rxn})	34	11		13		20	22
No. of trays in rectifying section (N_R)	1	9		13		4	2
Reactive trays	4–37	0–10		0–12		10–29	13–34
Acetic acid feed tray	36	0		0		25	30
Alcohol feed tray	13	0		0		29	34
Feed flow rate of acid (kmol/h)	50.00	48.40		48.20		50.00	50.00
Feed flow rate of alcohol (kmol/h)	50.00	50.00		50.00		50.00	50.00
Top product flow rate (kmol/h)	50.35	50.30		49.94		50.38	49.98
Bottom product flow rate (kmol/h)	49.65		48.10		48.26	49.62	50.02
X_D or $X_{D,aq}$							
Acid (m.f.)	0.00087	0.00001		2.5E-6		0.01670	0.00221
Alcohol (m.f.)	0.00556	0.02337		0.02665		0.00688	0.00643
Acetate (m.f.)	0.98000	0.01533		0.00835		0.00076	0.00019
Water (m.f.)	0.01357	0.96129		0.96500		0.97566	0.99117
X_B							
Acid (m.f.)	0.01237		0.00010		0.00002	0.00004	0.00711
Alcohol (m.f.)	0.00763		0.00912		0.00993	0.01006	0.00289
Acetate (m.f.)	$<10^{-8}$		0.99000		0.99000	0.98990	0.99000
Water (m.f.)	0.98000		0.00078		0.00005	$<10^{-8}$	$<10^{-8}$
Condenser duty (kW)	−1280.22	−4265.71	−1860.54	−3428.58	−1129.89	−2857.92	−1483.15
Subcooling duty (kW)		−833.82		−506.51		−461.35	−227.42
Reboiler duty (kW)	1035.71	4523.98	2195.68	3473.31	1370.90	3085.41	1532.48
Column diameter (m)	1.03	1.95	1.45	1.89	1.23	1.88	1.34
Weir height (m)	0.1016	0.1016	0.0508	0.1016	0.0508	0.0508	0.0508
TAC ($1000/year) (50 kmol/h)	374.14	1304.82		1051.56		753.28	482.54
TAC ($1000/year) (52825 ton/year)	659.14	2005.82		1388.46		850.20	482.54

distillation columns exhibit strong nonlinearity for all five systems studied, despite showing different degrees of severity. Moreover, the "sign reversal" is also observed for all five systems under either Q_R or FR change. The "sign reversal" indicates that the steady-state gain of a specific tray temperature changes sign as the magnitude of the same manipulated variables varies.

The results presented here are rather unconventional, because chemical processes are known to be quite nonlinear, but not to this degree in such a consistent manner. Two measures are used to differentiate the degree of nonlinearity for these three types of reactive distillation. One obvious choice is the faction of sign reversal for all tray temperatures. In this aspect, the AmAc system (Figure 3) indicates that more than half of the trays show sign reversal followed by the MeAc system (category I), in which almost half of the tray temperatures exhibit the "sign reversal." The category II system (EtAc and IPAc) show that almost 1/3 of the tray temperatures exhibit the "sign reversal" and the BuAc system is the system with the least sign changes in the tray temperatures. Table 2 summarizes the fraction of a sign changes for all five systems. The second nonlinearity indicator is ϕ^N, which was first proposed by Allgower[18] for general dynamic systems and further studied by Hernjak and Doyle[19] for systems under feedback. Schweickhardt and Allgower[20] give an updated summary on the nonlinearity measure. Here, we consider only the steady-state aspect (can be viewed as the nonlinearity measure for a static function) and the approach of Schweickhardt and Allgower[21] is taken here. In this work, the 2-norm is used to compute ϕ^N and each manipulated variable is considered separately. The measure is defined as

$$\phi^N = \inf_{G\in\cdot} \sup_{u\in\cdot} \frac{\|G(u) - N(u)\|_2}{\|N(u)\|_2} \tag{1}$$

Table 2. Fractions of Sign Reversal and Nonlinearity Measures for All Five Esterification Systems

Flowsheet Type	System	Fraction of Sign Reversal			Nonlinearity Measure (Schweickhardt and Allgower)			Overall Assessment†
		Q_R	FR	Overall*	Q_R	FR	Overall**	
I	MeAc	0.40	0.18	0.43	0.84	0.44	0.67	High
II	EtAc	0.03	0.40	0.43	0.34	0.70	0.55	Medium
	IPAc	0.03	0.29	0.32	0.32	0.60	0.48	Medium
III	BuAc	0.03	0.15	0.18	0.16	0.46	0.34	Low
	AmAc	0.30	0.57	0.76	0.78	0.79	0.79	High

*Delete overlapping (from each input) trays.
**Taking as 2-norm of two inputs divided by 2.
†High (if the averaged value >0.5), Medium (if the averaged value >0.3), and Low (if the averaged value <0.3).

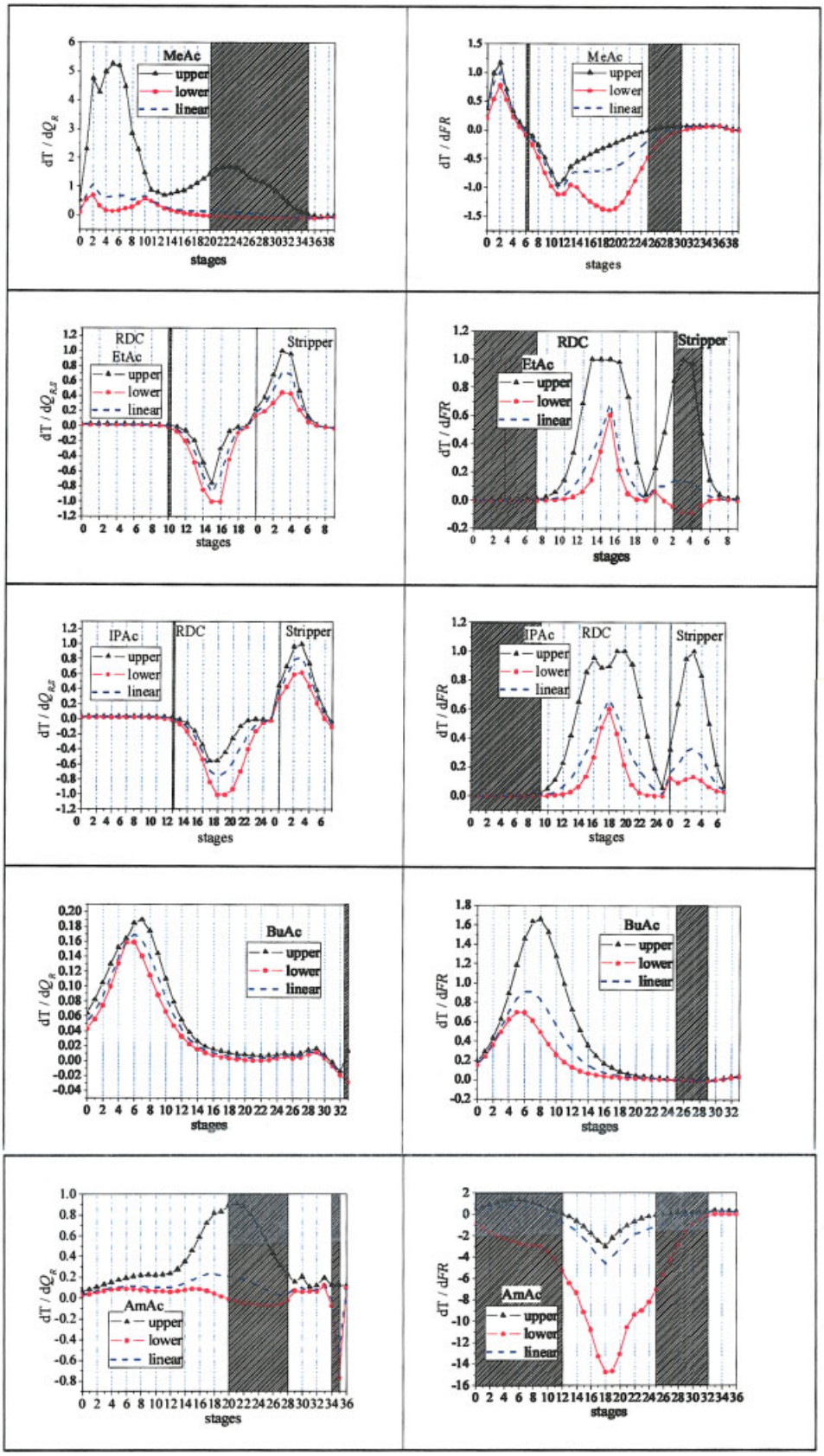

Figure 3. Upper and lower bounds of steady-state gains of all tray temperatures for ±5% reboiler duty and ±1% feed ratio changes and the sign reversal indicated as shaded areas.

[Color figure can be viewed in the online issue, which is available at www.interscience.wiley.com.]

where G is a linear operator, N is a nonlinear static function, $u \in \cdot$ is the input set, $G \in \cdot$ is a set of all linear operators. Physically, this can be viewed as the relative deviation of a linear (static) transfer function to the nonlinear function in a normalized sense. The measure ϕ^N ranges from 0 to 1 and $\phi^N = 0$ indicates a linear system and ϕ^N increases toward 1 as the nonlinearity becomes more severe. For static functions with the upper and lower bounds available, the solution to the optimization problem is simply

$$\frac{\|\bar{G} - G_+\|_2}{\|G_+\|_2} = \frac{\|\bar{G} - G_-\|_2}{\|G_-\|_2} \tag{2}$$

where G_+ is the upper bound of $N(\boldsymbol{u})/\boldsymbol{u}$ and G_- is the lower bound of $N(\boldsymbol{u})/\boldsymbol{u}$. By solving Eq. 2, the linear approximation $\bar{G}$ can be obtained as shown in Figure 3. Consequently, the nonlinear measure can be computed as

$$\phi^N = \frac{\|\bar{G} - G_+\|_2}{\|G_+\|_2} = \frac{\|\bar{G} - G_-\|_2}{\|G_-\|_2} \tag{3}$$

The vector G corresponds to tray temperatures throughout the column. Because we treat two manipulated inputs separately, two ϕ^N values are available for a given system. Table 2 gives the nonlinearity measures for all five systems with two different inputs. Qualitatively, the results of ϕ^N are consistent with the fractions of sign reversal as shown in Table 2. The 2-norm is used for overall nonlinearity assessment based on ϕ^N and the results are consistent with the previous "sign reversal" analysis. The ranking of the processes from linear to nonlinear becomes: BuAc (Type III) $\rightarrow$ IPAc (Type II) $\rightarrow$ EtAc (Type II) $\rightarrow$ MeAc (Type I) $\rightarrow$ AmAc (Type III).

In addition to the tray temperatures, we are also interested in the behavior of product composition for a range of changes in input. As indicated by Doherty and Malone[1] and Al-Arfaj and Luyben,[8] the MeAc system exhibits the "input multiplicity" where more than one set of inputs give the same outputs. Figure 4 clearly shows that either the heat input or the feed ratio results in the input multiplicity for the two products, MeAc and H_2O. The vertical dashed line in Figure 4 indicates the nominal steady state. From a separation perspective, an increase in the heat input will enrich the bottoms product, although Figure 4 indicates that H_2O composition goes through an increase followed by a decrease. Similarly, the top product composition, MeAc, also shows a nonmonotonic behavior as the heat input changes, and these unexpected results have also been observed for the feed ratio change (Figure 4). If a tray temperature T_{11} is used, instead of composition, the multiplicity problem can be alleviated only slightly, but cannot be eliminated completely. For the type II flowsheet, the input multiplicity occurs only between the feed ratio and the acetate composition as shown in Figure 4. Because the feeds are introduced to the reactive distillation column (RDC) and the product EtAc or IPAc is withdrawn from the stripper, this multiplicity will not affect process operation. Moreover, it is possible to find a tray temperature such that the input multiplicity can be eliminated (such as $T_{RDC,15}$ for EtAc and $T_{RDC,18}$ for IPAc) as shown in Figure 4. The two category III systems, again, show quite different process characteristics. Similar to the previous nonlinearity analysis, the BuAc system does not reveal any multiplicity; the AmAc system, on the other hand, shows the input multiplicity for the feed ratio variation. If a temperature, that is, T_{16}, is used instead, the input multiplicity cannot be eliminated completely. The multiplicity analysis indicates that the composition control of the MeAc system can be difficult and this is also true for the AmAc system where the input multiplicity cannot be completely eliminated. With respect to the type II flowsheets (EtAc and IPAc), the input multiplicity can be overcome by using the temperature control as shown in Figure 4. Similar to the previous analysis, the BuAc system does not show any potential problem in control.

The analysis presented here clearly indicates that the reactive distillation systems, regardless of types of flowsheet, exhibit severe nonlinearity, which includes a significant portion of the sign reversal, an extremely large value of Allgower's nonlinearity ϕ^N, and input multiplicity. Under these circumstances, control structure design and controller structure design become more important.

As shown in Figure 4, for the type II flowsheet, the "input multiplicity" can be avoided by controlling a tray temperature instead of product composition control. However, the problem cannot be avoided for the type I flowsheet for MeAc production. The problem then becomes: what kind of controllers can provide adequate control for such a nonlinear process?

Control Structure Design

In this section, a systematic approach is proposed to the control structure design for these three types of reactive distillation flowsheets. Because all five reactive distillation systems (Table 1) are of almost equal molar feed flows—a "neat" flowsheet—the stoichiometric balance has to be maintained.[15,16] In this work, the feed ratio (*FR*) is adjusted to prevent accumulation of unreacted reactants and stoichiometric imbalance. The next issue is: how many product compositions or inferred product purities should be controlled? For the esterification reactions with A + B $\leftrightarrow$ C + D under the "neat" flowsheet, controlling one-end product purity implied a similar purity level on the other end, provided with equally distributed product flow rates. So, a single-end composition (or temperature control) is preferred. This leads to 2×2 multivariable control, as opposed to a 3×3 multiple input/multiple-output (MIMO) system. The next problem concerns more of a robustness consideration. Because of input multiplicities and potential sign reversals, the uncertainty associated with a linear model can be significant. Instead of inverting all four transfer function models (for a 2×2 system) for controller design, a decentralized control is used where only information on the diagonal elements is used for initial design. In other words, the uncertainty associated with process is so large that we would like to minimize the exercise of model inversion. Thus, the decentralized control is preferred. In summary, the following principles are recommended:

(1) Maintain the stoichiometric balance using the feed ratio.

(2) Prefer to control only one-end composition (or temperature).

(3) Use decentralized control to maintain robust stability.

This leads to the following design procedure for temperature control of reactive distillation systems.

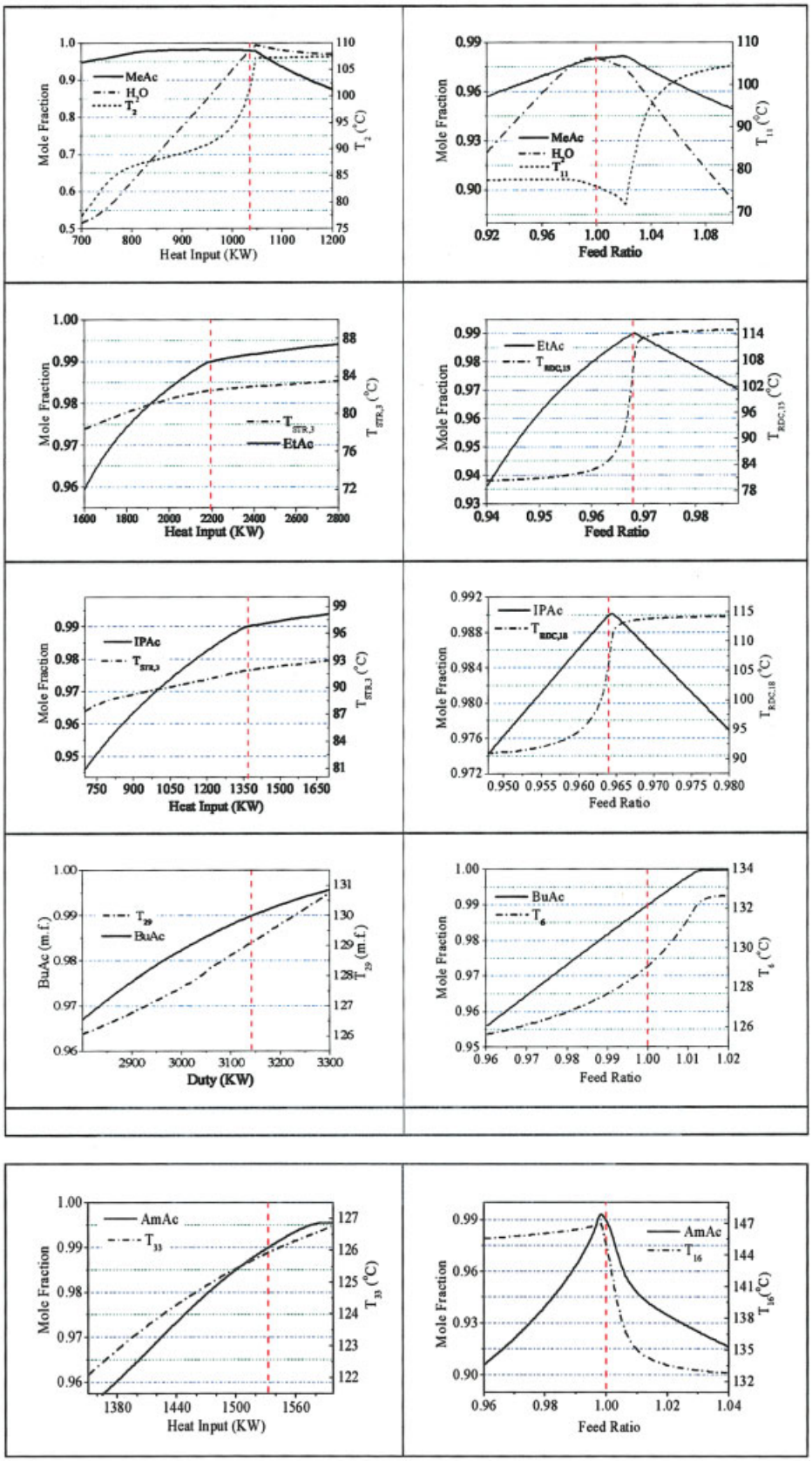

Figure 4. Trends of product compositions and temperature responses for a range of changes in the manipulated variables (heat input and feed ratio) and nominal design indicated by the dashed line.

[Color figure can be viewed in the online issue, which is available at www.interscience.wiley.com.]

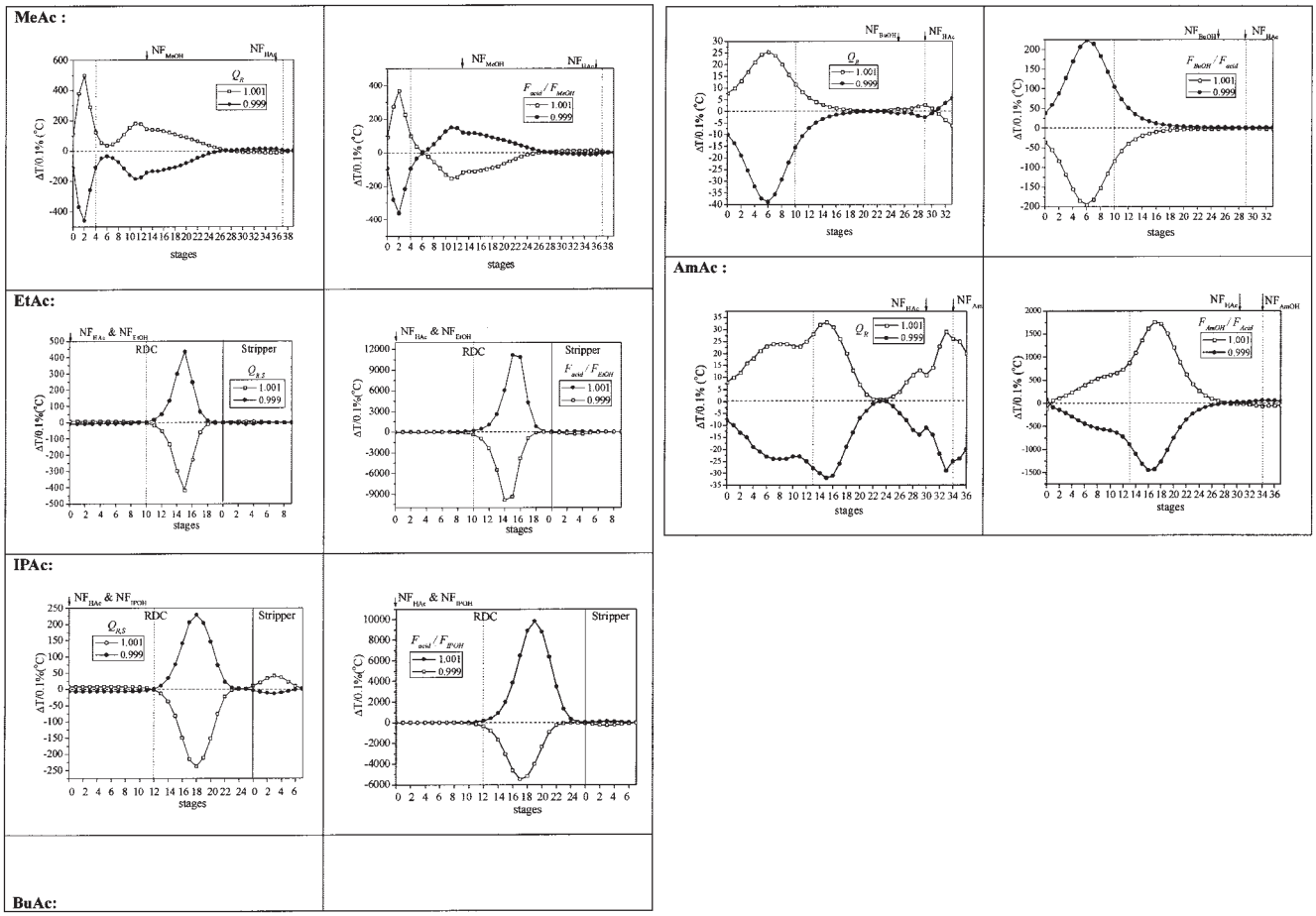

Figure 5. Sensitivities of tray temperatures for ±0.1% manipulated variables changes and reactive zone indicated by two dotted lines.

(1) Select an additional manipulated variable. Typically, the other manipulated input is the heat input or the reflux ratio.

(2) Use the nonsquare relative gain (NRG[22]) to select temperature control trays. The larger row sums of the NRG indicate potential temperature control tray. Note that the temperatures with the "sign reversal" (Figure 3) cannot be used as controlled variable.

(3) Use the relative gain array (RGA) for variable pairing, once the inputs and outputs are determined.

(4) Perform a sequential relay feedback test[23] to find the ultimate gain (K_u) and ultimate period (P_u).

(5) Use the Tyreus–Luyben tuning to set the tuning constant for the PI controllers. A simple version is: $K_c = K_u/3$ and $\tau_I = 2P_u$.

Selection of temperature control trays

Sensitivity analyses are performed on these five esterification reactive distillation systems (Table 1). To find the steady-state gains of tray temperature in the linear region, extremely small step changes (±0.1%) in the manipulated variables are made.

For the MeAc system (Figure 1A), a step increase in the heat input (Q_R) leads to temperature increase in the lower section of the column and a relatively small temperature decrease toward the top of the column as shown in Figure 5. This is uncharacteristic because, for conventional distillation, we generally observe temperature increases throughout the column. For the change in the second manipulated variable (acid feed flow rates over alcohol feed rate, $F_{Acid}/F_{Alcohol}$), an increase in the flow rate of the heavy reactant (F_{Acid}) results in a temperature increase in the lower section of the column, followed by a decrease toward the middle section of the column (Figure 5). The reason for the temperature increase in the lower section is explained by the excess of the heavy reactant (HAc). Because of the lowered conversion, less water (the second highest boiler) is formed and, subsequently, leads to a lower tray temperature in the midsection of the column.

The type II flowsheet shows a different configuration where the base level of the reactive distillation column (RDC) is controlled by the heat input (a dependent variable) and the heat input of the stripper ($Q_{R,S}$) is the manipulated variable as shown in Figure 1B. The second manipulated variable is the feed ratio and the reflux ratio of the RDC is fixed. For the EtAc system, an *increase* in $Q_{R,S}$ leads to a *decrease* in the tray temperatures of the reactive distillation column (Figure 5). Note that in Figure 5 the temperatures in the RDC and the stripper are combined and are labeled in the *x*-axis. This is a rather unusual phenomenon, which is a direct consequence of the process

configuration. An increase in $Q_{R,S}$ results in a larger vapor rate from the stripper back to the decanter and this implies a larger recycle flow rate for the reactive distillation column. As for the acid feed ($F_{Acid}/F_{Alcohol}$) changes, an increase in the heavy reactant results in the RDC tray temperature rise, whereas the stripper temperatures show little variation. The arguments also apply to the IPAc system as shown in Figure 5.

Topographically, the type III flowsheet is quite similar to the type I flowsheet, except that a decanter is used to replace the condenser and the organic phase is totally refluxed (Figure 1). For the BuAc system, an increase in the heat input leads to the temperature rise throughout the column except for the upper section of the column, which is quite similar to the MeAc system. In the column design, the HAc concentration is kept low toward the lower section of the column[15] to meet product specification (acid in ppm level). Thus, an increase in the acid feed rate increases the formation of BuAc in the lower section and results in a higher tray temperature as shown in Figure 5. Because of the close boiling of two reactants and feed arrangement, the acid is consumed early in the reactive zone and the trend of temperature decrease is observed, although not as significant as that of the MeAc system. Similar behavior can also be seen for the AmAc system, except that the heavy reactant is the alcohol (AmOH) instead of the acid (HAc) as can be seen in Figure 5.

The nonsquare relative gain (NRG) of Chang and Yu[22] is used to find the temperature control trays. The NRG (Λ^N) is defined as

$$\Lambda^N = K_p \otimes (K_p^+)^T \tag{4}$$

where K_p is the steady-state gain matrix, $\otimes$ denotes the element-by-element multiplication, the superscript $+$ is the pseudoinverse, and the superscript T means the transpose. The largest row sum of the NRG is selected as the temperature control trays. Figure 6 shows the row sums for all five systems and thus the controlled variables are as follows:

- MeAc: T_2 and T_{11}
- EtAc: $T_{RDC,15}$ and $T_{STR,3}$
- IPAc: $T_{RDC,18}$ and $T_{STR,3}$
- BuAc: T_6 and T_{29}
- AmAc: T_{11} and T_{33}

Because the NRG is a linear analysis, the nonlinearity measure for each individual tray (ϕ) is also computed (Figure 6) to evaluate potential conflict between linear and nonlinearity analyses. Note that ϕ, shown here, is obtained by taking the 2-norm of individual nonlinearity measure from each input and then dividing by 2. The nonlinear results are generally in good agreement with the linear results, except for the BuAc case where the trays close to the column top are not used to avoid poor mixing. It is also important to ensure that the selected temperature control trays do not exhibit sign changes when manipulated inputs are varied (Figure 3). The shaded areas in Figure 3 indicate that, for these five systems, the temperature control trays do not exhibit sign reversal in the ranges ($\pm 5\%$ for Q_R and $\pm 1\%$ for FR) of manipulated variable variations. Note that if the NRG selected temperature falls within the "sign reversal" area, an alternative temperature should be sought.

Control structure and controller design

Because we choose to use the decentralized control for highly nonlinear reactive distillation systems, the next step is to find the variable pairing for the controlled and manipulated variables. Table 3 (fourth column) gives the steady-state gain matrices from the linear analysis. The relative gain array (RGA[25]) is used for variable pairings. The selected pairings (fifth column of Table 3) give diagonal RGAs ranging from 0.53 to 1.04. For the MeAc system, the heat input is used to control T_2 and T_{11} is maintained by changing the feed ratio (that is, T_2–Q_R and T_{11}–FR), which looks reasonable from a dynamical perspective (note that we are counting the tray number from bottoms up). For the type II flowsheets (EtAc and IPAc), a stripper temperature is maintained using the heat input to the stripper and a temperature in the RDC is controlled using the ratio of fresh feeds into the RDC (that is, $T_{STR,3}$–$Q_{R,S}$ and $T_{RDC,15}$–FR for EtAc and $T_{STR,3}$–$Q_{R,S}$ and $T_{RDC,18}$–FR for IPAc). The control structures for the type III flowsheet may look odd from the conventional distillation control perspective, but they have been seen frequently for reactive distillation.[26,27] Here, the heat input is paired with an upper section tray temperature and a lower section tray temperature is controlled by the feed ratio (such as T_{29}–Q_R and T_6–FR for BuAc and T_{33}–Q_R and T_{16}–FR for AmAc). The relay feedback test[23] is used to find the ultimate gain (K_u) and the ultimate period (P_u) followed by the Tyreus–Luyben PI tuning rule. The identification-tuning step is carried out sequentially to find the controller settings for the PI controller. We find the sequential relay feedback autotuning procedure is very effective for these five highly nonlinear processes. Table 3 summarizes the settings for all five reactive systems with two PI loops. It can be seen that the large reset time is associated with the FR loop and the reset time for the heat input loop is relatively small. This implies we have two dynamically different speeds of response. The heat input loop takes care of the disturbance initially followed by a gradual effort to maintain the stoichiometric balance (to prevent gradual accumulation).

Performance

Feed flow and feed ratio disturbances are used to evaluate the control performance of the temperature control for these five esterification systems. Recall that these reactive distillation systems are highly nonlinear (Figure 3) with significant "sign reversal" and input multiplicity. Figure 7 shows that the simple PI temperature control actually works quite well for all five systems.

For the MeAc system, two temperature control trays (T_2 and T_{11}) show asymmetric responses and oscillatory behavior is observed for T_{11} (Figure 7A). The product composition, $X_{D,acetate}$ in particular, does not settle down 15 h after the 20% feed flow rate change is introduced. Asymmetrical responses are observed for most of the process variables and steady-state offsets ($\sim$0.002 m.f.) exist (Figure 7A). For the type II flowsheets, faster responses and many symmetrical responses can be obtained for the controlled temperatures as well as major product compositions as shown in Figures 7B and 7C. The product composition settles in $<$10 h and much smaller offsets in the acetate composition can be achieved ($\sim$0.001 m.f. for EtAc and nil for IPAc). For the type III flowsheets, symmetrical responses in the temperature control trays can be seen in

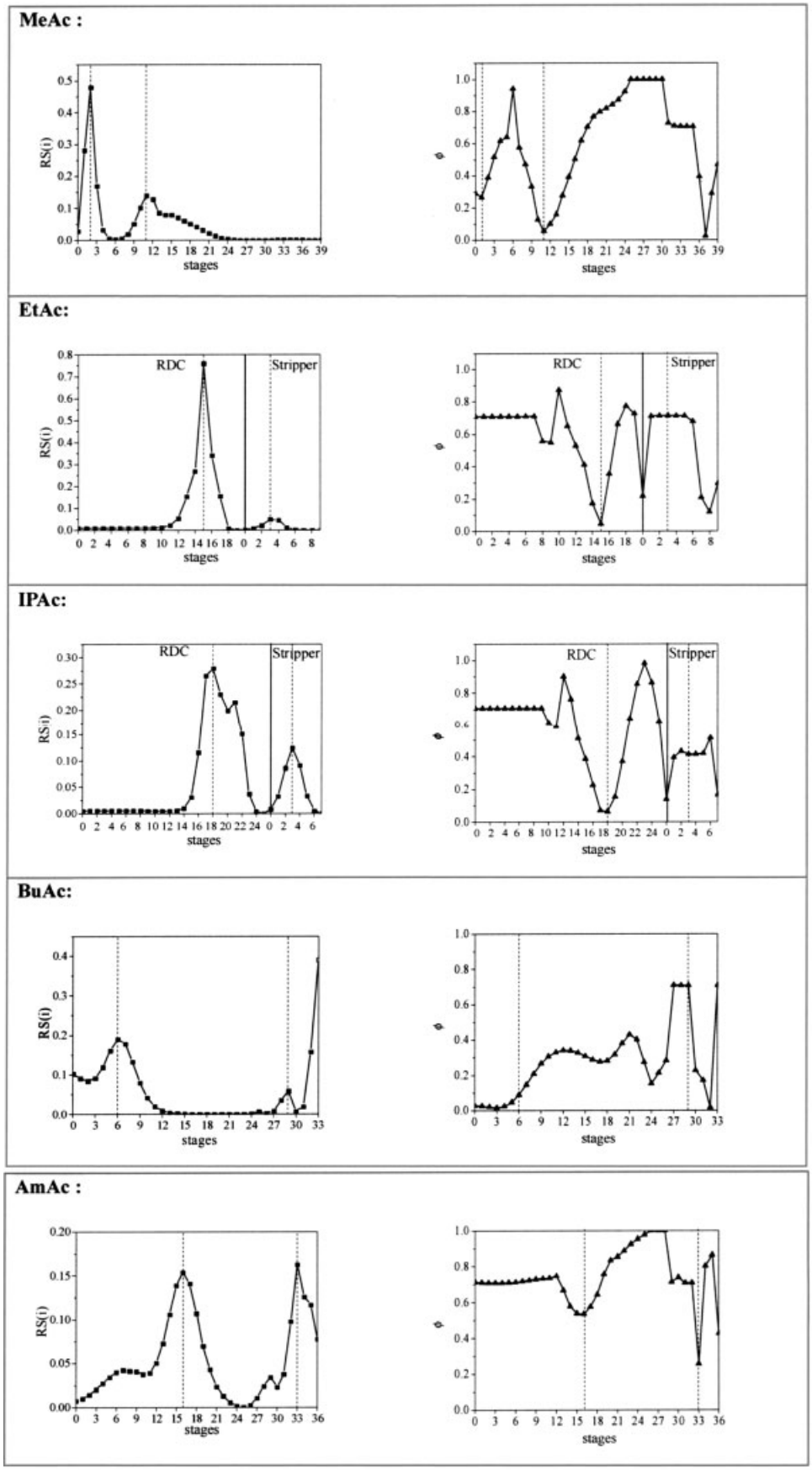

Figure 6. Row sums and nonlinearity measures (ϕ) of individual tray temperature for all five systems.

Table 3. Controlled Variables, Manipulated Variables, Process Gain Matrices, Relative Gain Array, and Tuning Parameters for These Five Esterification Systems under Temperature Control

System	Controlled Variables	Manipulated Variables	Steady-State Gain	RGA	Tuning Parameter
MeAc	T_2 T_{11}	F_{Acid}/F_{MeOH} Q_R	$\begin{bmatrix} T_{11} \\ T_2 \end{bmatrix} = \begin{bmatrix} 1.839 & -1.522 \\ 4.802 & 3.659 \end{bmatrix} \begin{bmatrix} Q_R \\ F_{Acid}/F_{MeOH} \end{bmatrix}$	$\Lambda = \begin{matrix} Q_R \\ \\ T_{11} \\ T_2 \end{matrix} \begin{matrix} F_{Acid}/F_{MeOH} \\ \begin{bmatrix} 0.479 & 0.520 \\ 0.520 & 0.479 \end{bmatrix} \end{matrix}$	Q_R–T_2: $K_c = 0.464$ $\tau_I = 0.333$ (h) F_{Acid}/F_{MeOH}–T_{11}: $K_c = 1.237$ $\tau_I = 1.98$ (h)
EtAc	$T_{STR,3}$ $T_{RDC,15}$	F_{Acid}/F_{EtOH} $Q_{R,S}$	$\begin{bmatrix} T_{STR,3} \\ T_{RDC,15} \end{bmatrix} = \begin{bmatrix} 0.087 & 1.967 \\ -4.26 & 102.57 \end{bmatrix} \begin{bmatrix} Q_{R,S} \\ F_{Acid}/F_{EtOH} \end{bmatrix}$	$\Lambda = \begin{matrix} Q_{R,S} \\ \\ T_{STR,3} \\ T_{RDC,15} \end{matrix} \begin{matrix} F_{Acid}/F_{EtOH} \\ \begin{bmatrix} 0.517 & 0.482 \\ 0.482 & 0.517 \end{bmatrix} \end{matrix}$	$Q_{R,S}$–$T_{STR,3}$: $K_c = 22.65$ $\tau_I = 0.018$ (h) F_{Acid}/F_{EtOH}–$T_{RDC,15}$: $K_c = 0.755$ $\tau_I = 2.069$ (h)
IPAc	$T_{STR,3}$ $T_{RDC,18}$	F_{Acid}/F_{IPOH} $Q_{R,S}$	$\begin{bmatrix} T_{STR,3} \\ T_{RDC,18} \end{bmatrix} = \begin{bmatrix} 0.227 & 1.574 \\ -2.336 & 70.439 \end{bmatrix} \begin{bmatrix} Q_{R,S} \\ F_{Acid}/F_{IPOH} \end{bmatrix}$	$\Lambda = \begin{matrix} Q_{R,S} \\ \\ T_{STR,3} \\ T_{RDC,18} \end{matrix} \begin{matrix} F_{Acid}/F_{IPOH} \\ \begin{bmatrix} 0.812 & 0.187 \\ 0.187 & 0.812 \end{bmatrix} \end{matrix}$	$Q_{R,S}$–$T_{STR,3}$: $K_c = 25.5$ $\tau_I = 0.08$ (h) F_{Acid}/F_{IPOH}–$T_{RDC,18}$: $K_c = 3.92$ $\tau_I = 2.66$ (h)
BuAc	T_{29} T_6	F_{BuOH}/F_{Acid} Q_R	$\begin{bmatrix} T_{29} \\ T_6 \end{bmatrix} = \begin{bmatrix} 0.026 & -0.007 \\ 0.299 & -2.127 \end{bmatrix} \begin{bmatrix} Q_R \\ F_{BuOH}/F_{Acid} \end{bmatrix}$	$\Lambda = \begin{matrix} Q_R \\ \\ T_{29} \\ T_6 \end{matrix} \begin{matrix} F_{BuOH}/F_{Acid} \\ \begin{bmatrix} 1.041 & -0.041 \\ -0.041 & 1.041 \end{bmatrix} \end{matrix}$	Q_R–T_{29}: $K_c = 38.86$ $\tau_I = 0.06$ (h) F_{BuOH}/F_{Acid}–T_6: $K_c = 5.16$ $\tau_I = 0.9$ (h)
AmAc	T_{33} T_{16}	F_{AmOH}/F_{Acid} Q_R	$\begin{bmatrix} T_{33} \\ T_{16} \end{bmatrix} = \begin{bmatrix} 0.29 & -0.059 \\ 0.31 & 15.995 \end{bmatrix} \begin{bmatrix} Q_R \\ F_{AmOH}/F_{Acid} \end{bmatrix}$	$\Lambda = \begin{matrix} Q_R \\ \\ T_{33} \\ T_{16} \end{matrix} \begin{matrix} F_{AmOH}/F_{Acid} \\ \begin{bmatrix} 0.961 & 0.038 \\ 0.038 & 0.961 \end{bmatrix} \end{matrix}$	Q_R–T_{33}: $K_c = 29.72$ $\tau_I = 0.08$ (h) F_{AmOH}/F_{Acid}–T_{16}: $K_c = 9.1$ $\tau_I = 1.2$ (h)

* Transmitter span: twice of steady-state value of temperature in °C.
**Valve gains: twice of the steady-state value for Q_R ($Q_{R,S}$) and FR.

Figures 7D and 7E. However, two different composition dynamics are observed that can be foreseen from nonlinear analysis (Table 2). For the BuAc system, the product composition dynamics settles in <5 h (the fastest response) and symmetrical responses can also been seen for most of the process variables except the trace acid concentration (Figure 7D). Steady-state offsets are also observed, but error is around 0.002 m.f. for ±20% feed flow changes. For the AmAc system, again, fast dynamics is attainable, but the responses are asymmetrical, especially for the product compositions $X_{B,acetate}$ and X_{D,H_2O}. Large steady-state offset (~0.02 m.f.) is also observed for the acetate composition.

The second disturbance explored is ±5% FR changes. It can be viewed as steplike flow measurement errors (such as bias). Figure 8 shows the control performance for ±5% FR disturbances. Generally, offset free composition control can be achieved by holding two temperatures at their set points. As shown in Figure 8, the speed of responses for each system is quite similar to that of the feed flow disturbances. The MeAc system takes >15 h to settle while showing significant nonlinearity (Figure 8A). The EtAc and IPAc systems take about 10 h to return to steady state with almost negligible error in the product (acetate) composition (Figures 8B and 8C). The BuAc and AmAc systems give the fastest dynamics and the product compositions return to set point in about 5 h as shown in Figures 8D and 8E. For the AmAc system, the feed ratio disturbance is much better handled, as compared to the feed flow changes (Figure 7E).

Despite the strong nonlinearity (Figures 4 and 5), workable temperature control of esterification reactive distillation systems can be obtained using a systematic design procedure with a rather simple control structure. It should be emphasized that the selections of controlled and manipulated variables (control structure design) play a crucial role for these highly nonlinear processes and the decentralized control provides a better structure to cope with steady-state gain variations. Table 4 states the control performance qualitatively for these five systems. As expected, the MeAc system (type I flowsheet) exhibits relatively poor control performance as can be seen early from qualitative (saddle) argument or quantitative nonlinearity measures. The closed-loop behavior of the EtAc and IPAc (type II flowsheet) is not quite as nonlinear as the steady-state measures predict. Relatively fast and symmetrical dynamics can be obtained as shown in Figures 7B, 7C, 8B, and 8C. One reason for this is that the type II flowsheet has a two-column configuration (Figure 1) and they are separated by a decanter, typically with a 20-min holdup. In other words, a large surge tank is placed between these two units and they are somewhat decoupled dynamically. As predicted, the BuAc system should be an easy one to control and the closed-loop responses confirmed that (Figures 7D and 8D).

The other type III flowsheet, the AmAc system, on the other hand, gives significantly different closed-loop performance. Fewer symmetrical responses are observed as predicted by the nonlinearity measures and a large composition offset results for feed flow rate changes (Figure 7E). However, similar to the BuAc system, the type III flowsheet generally gives fast closed-loop dynamics. Table 4 summarizes the performance, settling time, and steady-state errors in product composition, for these five temperature-controlled reactive distillation systems. The results given in Table 4 are for ±20% feed flow changes. Note that control performance (such as the MeAc system in Figure 7A) can be improved by incorporating feedforward control for measured disturbance. For example, we can ratio the feed flow rate to the reboiler duty for better control performance for the MeAc system.

Finally, it is interesting to note that the two systems (MeAc and AmAc) with lower total annual cost (TAC) give relatively poor closed-loop responses in either slow dynamics or large

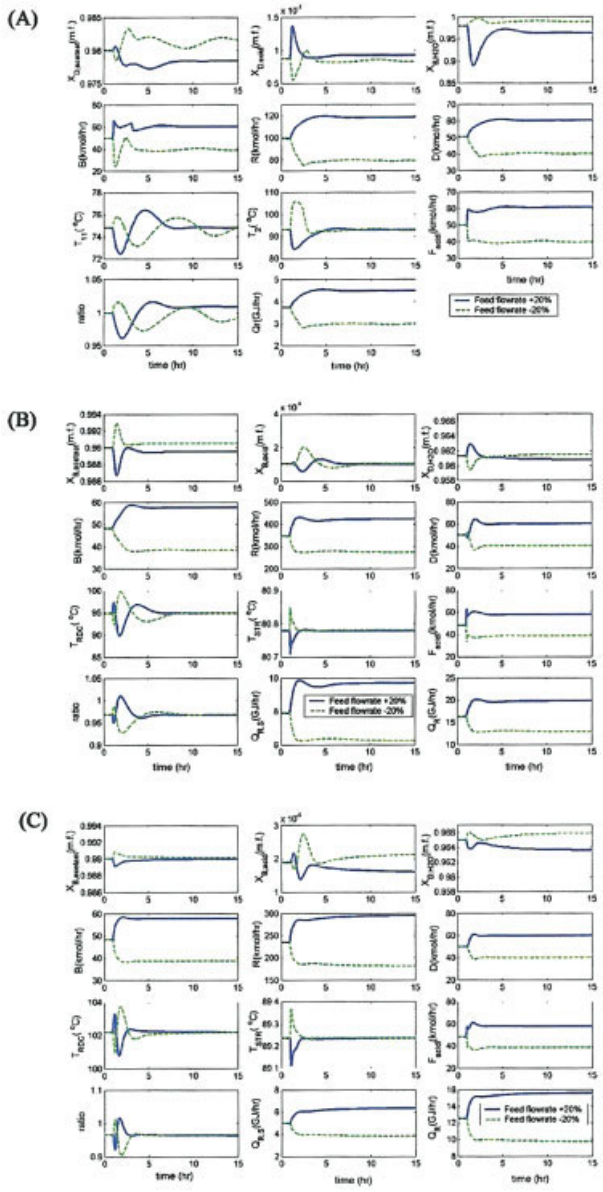

Figure 7. Temperature control responses for ±20% production rate changes for (A) MeAc, (B) EtAc, (C) IPAc, (D) BuAc, and (E) AmAc systems.

[Color figure can be viewed in the online issue, which is available at www.interscience.wiley.com.]

steady-state offset. Table 1 also gives the TACs for these five designs.

Extension to Composition Control

Because of the steady-state offsets in the temperature control, one may seek for the offset-free composition control in acetic acid esterification. With consideration of the reaction nature (same amount of C and D are produced in the A + B ↔ C + D) and maintenance, we could like to keep the number of composition loops to a minimal level. Here, we choose to control the purity level of the acetate product, except for the MeAc system.

In the previous section, two temperature control trays are

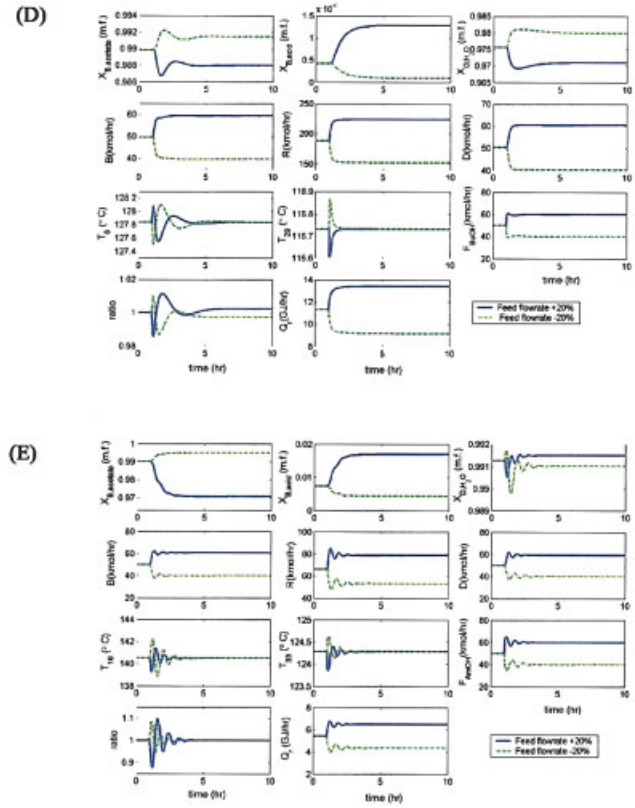

Figure 7. Continued.

selected from the NRG analysis. Because the bottoms product composition is one of the controlled variables, the other controlled variable is the temperature further away from the acetate withdrawal ends. The fourth column of Table 5 gives the steady-state gain matrices of these five 2 × 2 systems. One temperature and one composition are controlled with two manipulated variables: heat input and feed ratio.

Next, the relative gain arrays are computed for variable pairings. The results show that, for type I (MeAc) and type II (EtAc and IPAc) flowsheets, the composition is controlled with the heat inputs and the feed ratio is used for temperature control. For type III flowsheets (BuAc and AmAc), however, the acetate composition is maintained by changing the feed ratio and the tray temperature is controlled using the heat input (Table 5). The variable pairings in Table 5 indicate that severe nonlinearity will be encountered for the MeAc system and possibly also the AmAc system. The multiplicity analysis in Figure 4 reveals that, for the MeAc system, that both input–output pairs (X_{B,H_2O}–Q_R and T_{11}–FR) show input multiplicity and, for the AmAc system, the $X_{B,AmAc}$–FR pair also exhibits input multiplicity. The accompanying difficult control problem cannot be prevented, if we choose to control product composition for the MeAc system.

Once the controller structure is determined, the sequential relay feedback tests and autotuning are performed to find the PI controller settings as shown in Table 5. Similar to the settings for temperature control (Table 3), we have large reset times associated with the feed ratio and much smaller reset times for the heat input. Again, the control systems are designed in a systematic manner with a minimal complexity in the design steps, identification, tuning, and controller types.

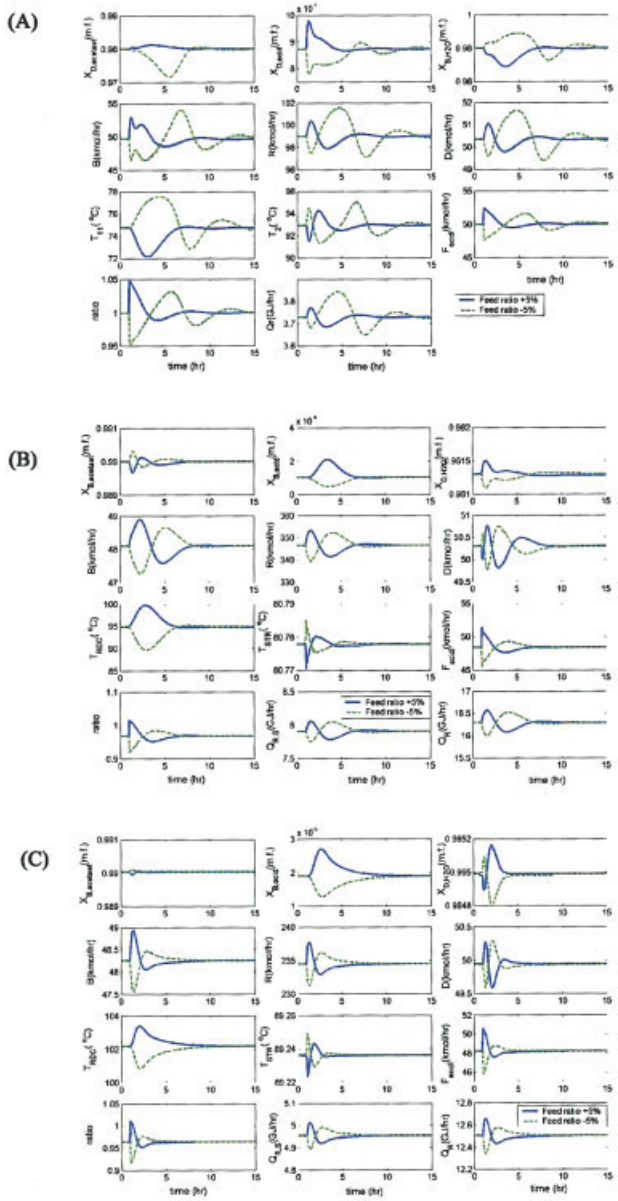

Figure 8. Temperature control responses for ±5% feed ratio changes for (A) MeAc, (B) EtAc, (C) IPAc, (D) BuAc, and (E) AmAc systems.

[Color figure can be viewed in the online issue, which is available at www.interscience.wiley.com.]

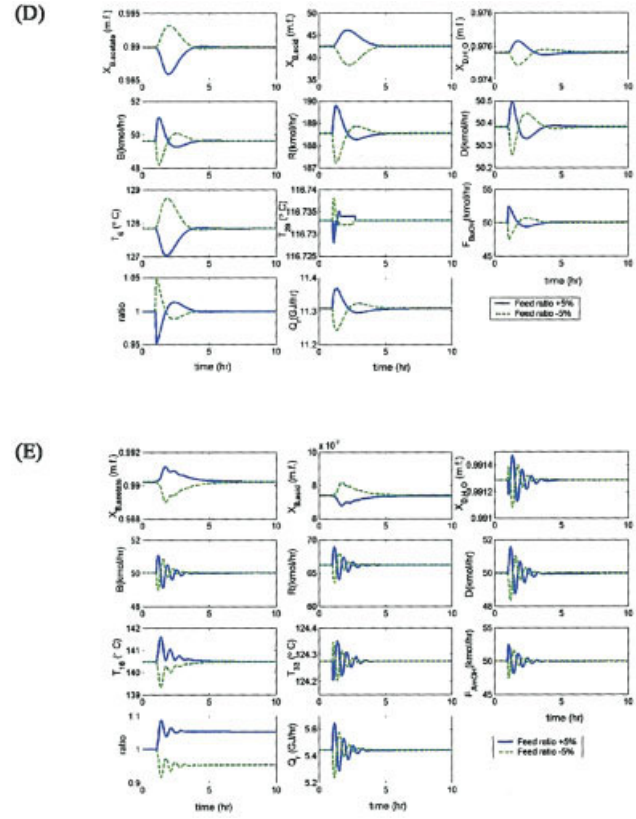

Figure 8. Continued.

The performance of the one-temperature/one-composition control is evaluated using Aspen Dynamics. For the composition measurement, 4 min of analyzer dead time is assumed. In general, the dynamic behaviors of these five systems under composition control are quite similar to that of the temperature control (Figure 9). For example, the MeAc and AmAc systems also show significant nonlinearity for feed flow rate disturbances and, on the other hand, relatively symmetric responses are observed for the EtAc, IPAc, and BuAc systems. Certainly, the steady-state offset in the acetate composition can be eliminated when a composition loop is in place. For the MeAc system, the peak error of the composition control is 20 times greater than that of the temperature control (Figures 7A and 9A) for a 20% feed rate decrease and good disturbance rejection can be achieved for a feed rate increase. For the EtAc and IPAc systems (type II flowsheet), only slight differences in the speed of response, peak error, and steady-state offsets are observed (Figures 7B, 7C, 9B, and 9C). So, there is little incentive to attempt composition control for the type II flowsheet. For the BuAc system, good control performance is possible using the composition control. The peak errors for the temperature and composition control are roughly the same except that offset-free product composition can be obtained (Figures 7D and 9D). Thus the composition control may be an attractive alternative for the BuAc system. For the AmAc system, the peak errors are almost the same for both the temperature control and composition control. However, the steady-state offset can be eliminated using one composition loop. This is another likely system to consider the composition control (Figures 7E and 9E). However, asymmetrical responses

Table 4. Dynamic Performance for Both Control Structures under ±20% Feed Flow Changes

		Dual-Temperature Control		One-Temperature/One-Composition Control	
Flowsheet Type	System	Settling Time (h)	Offset (m.f.)	Settling Time (h)	Peak Errors (m.f.)
I	MeAc	~15	~0.002	~10	~0.05
II	EtAc	~10	~0.001	~5	~0.005
	IPAc	~10	~0.001	~5	~0.005
III	BuAc	~5	~0.002	<5	~0.002
	AmAc	~5	~0.02	~10	~0.02

Table 5. Controlled Variables, Manipulated Variables, Process Gain Matrices, Relative Gain Array, and Tuning Parameters for These Five Esterification Systems under One-Temperature/One-Composition Control

System	Controlled Variables	Manipulated Variables	Steady-State Gain	RGA	Tuning Parameter
MeAc	$X_{B,\mathrm{H_2O}}$ T_{11}	F_{Acid}/F_{MeOH} Q_R	$\begin{bmatrix} X_{B,\mathrm{H_2O}} \\ \mathrm{T}_{11} \end{bmatrix} = \begin{bmatrix} 1.281 & -0.168 \\ 0.874 & -1.520 \end{bmatrix} \begin{bmatrix} Q_R \\ F_{Acid}/F_{MeOH} \end{bmatrix}$	$\Lambda = \begin{matrix} Q_R \\ \\ X_{B,\mathrm{H_2O}} \\ \mathrm{T}_{11} \end{matrix} \begin{bmatrix} 1.082 & -0.082 \\ -0.082 & 1.082 \end{bmatrix} \begin{matrix} F_{Acid}/F_{MeOH} \\ \\ \end{matrix}$	Q_R–$X_{D,\mathrm{H_2O}}$: $K_c = 1.8 \quad \tau_I = 0.316$ (h) F_{Acid}/F_{MeOH}–T_{11}: $K_c = 0.67 \quad \tau_I = 4.2$ (h)
EtAC	$X_{B,\mathrm{EtAc}}$ $\mathrm{T}_{\mathrm{RDC},15}$	F_{Acid}/F_{EtOH} Q_R	$\begin{bmatrix} X_{B,\mathrm{EtAc}} \\ \mathrm{T}_{\mathrm{RDC},15} \end{bmatrix} = \begin{bmatrix} 0.068 & 0.572 \\ -4.26 & 102.57 \end{bmatrix} \begin{bmatrix} Q_{R,S} \\ F_{Acid}/F_{EtOH} \end{bmatrix}$	$\Lambda = \begin{matrix} Q_{R,S} \\ \\ X_{B,\mathrm{EtAc}} \\ \mathrm{T}_{\mathrm{RDC},15} \end{matrix} \begin{bmatrix} 0.742 & 0.258 \\ 0.258 & 0.742 \end{bmatrix} \begin{matrix} F_{Acid}/F_{EtOH} \\ \\ \end{matrix}$	$Q_{R,S}$–$X_{B,\mathrm{EtAc}}$: $K_c = 14.05 \quad \tau_I = 0.64$ (h) F_{Acid}/F_{EtOH}–$\mathrm{T}_{\mathrm{RDC},15}$: $K_c = 0.755 \quad \tau_I = 2.069$ (h)
IPAc	$X_{B,\mathrm{IPAc}}$ $\mathrm{T}_{\mathrm{RDC},18}$	F_{Acid}/F_{IPOH} Q_R	$\begin{bmatrix} X_{B,\mathrm{IPAc}} \\ \mathrm{T}_{\mathrm{RDC},18} \end{bmatrix} = \begin{bmatrix} 0.1514 & 0.7013 \\ -2.336 & 70.439 \end{bmatrix} \begin{bmatrix} Q_{R,S} \\ F_{Acid}/F_{IPOH} \end{bmatrix}$	$\Lambda = \begin{matrix} Q_{R,S} \\ \\ X_{B,\mathrm{IPAc}} \\ \mathrm{T}_{\mathrm{RDC},18} \end{matrix} \begin{bmatrix} 0.866 & 0.133 \\ 0.133 & 0.866 \end{bmatrix} \begin{matrix} F_{Acid}/F_{IPOH} \\ \\ \end{matrix}$	$Q_{R,S}$–$X_{B,\mathrm{IPAc}}$: $K_c = 13.8 \quad \tau_I = 0.32$ (h) F_{Acid}/F_{IPOH}–$\mathrm{T}_{\mathrm{RDC},18}$: $K_c = 3.92 \quad \tau_I = 2.66$ (h)
BuAc	T_{29} $X_{B,BuAc}$	F_{BuOH}/F_{ACid} Q_R	$\begin{bmatrix} X_{B,BuAc} \\ \mathrm{T}_6 \end{bmatrix} = \begin{bmatrix} 2.785 & -19.043 \\ 0.026 & -0.007 \end{bmatrix} \begin{bmatrix} Q_R \\ F_{BuOH}/F_{Acid} \end{bmatrix}$	$\Lambda = \begin{matrix} Q_R \\ \\ X_{B,BuAc} \\ \mathrm{T}_{29} \end{matrix} \begin{bmatrix} -0.042 & 1.042 \\ 1.042 & -0.042 \end{bmatrix} \begin{matrix} F_{BuOH}/F_{Acid} \\ \\ \end{matrix}$	Q_R–T_{29}: $K_c = 21.8 \quad \tau_I = 0.06$ (h) F_{BuOH}/F_{Acid}–$X_{B,BuAc}$: $K_c = 6.43 \quad \tau_I = 5.04$ (h)
AmAc	T_{33} $X_{B,AmAc}$	F_{AmOH}/F_{Acid} Q_R	$\begin{bmatrix} X_{B,AmAc} \\ \mathrm{T}_{33} \end{bmatrix} = \begin{bmatrix} 2.337 & 55.721 \\ 0.29 & -0.595 \end{bmatrix} \begin{bmatrix} Q_R \\ F_{AmOH}/F_{Acid} \end{bmatrix}$	$\Lambda = \begin{matrix} Q_R \\ \\ X_{B,BuAc} \\ \mathrm{T}_{33} \end{matrix} \begin{bmatrix} 0.0792 & 0.920 \\ 0.920 & 0.079 \end{bmatrix} \begin{matrix} F_{AmOH}/F_{Acid} \\ \\ \end{matrix}$	Q_R–T_{33}: $K_c = 28.9 \quad \tau_I = 0.08$ (h) F_{AmOH}/F_{Acid}–$X_{B,\mathrm{AmAc}}$: $K_c = 0.92 \quad \tau_I = 24.4$ (h)

* Transmitter spans: twice of steady-state value of temperature and 1 for mole fraction.
**Valve gains: twice of the steady-state value for $Q_R(Q_{R,S})$ and FR.

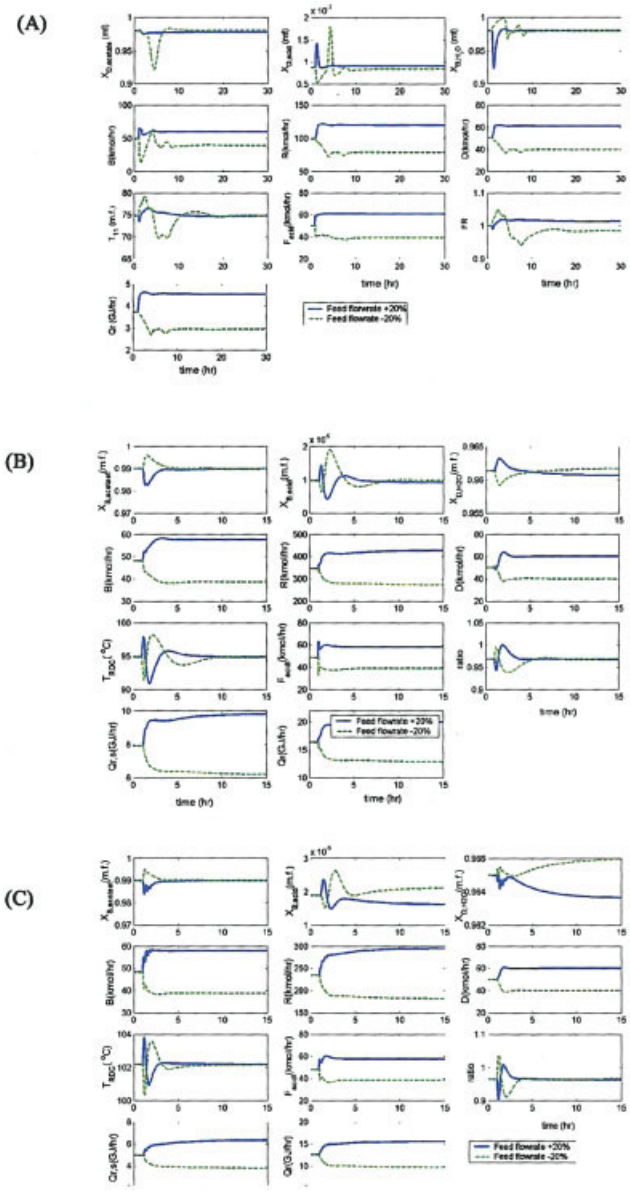

Figure 9. Composition control responses for ±20% production rate changes for (A) MeAc, (B) EtAc, (C) IPAc, (D) BuAc, and (E) AmAc systems.

[Color figure can be viewed in the online issue, which is available at www.interscience.wiley.com.]

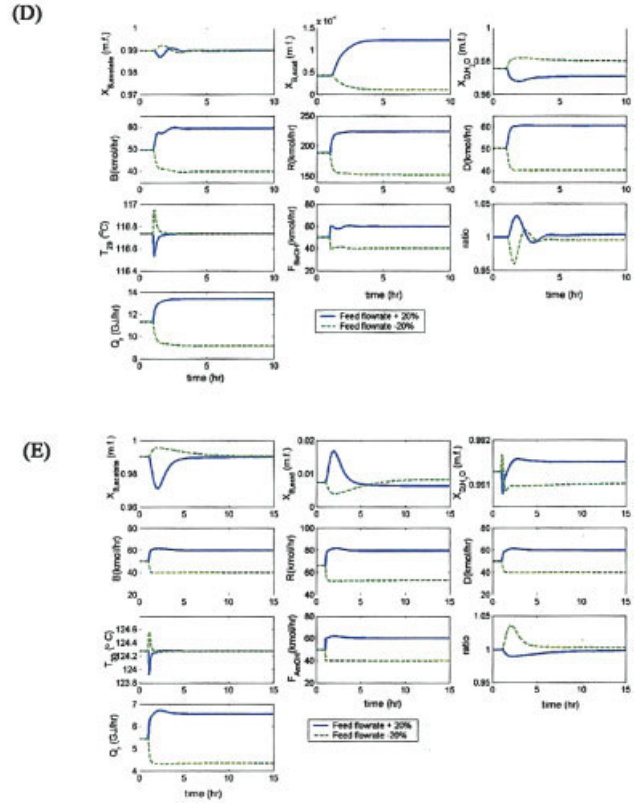

Figure 9. Continued.

can also be seen for the AmAc system. For the feed ratio disturbances, the EtAc, IPAc, and BuAc systems are symmetrical with acceptable speeds of responses (Figure 10). Again, oscillatory behaviors are observed for the MeAc (Figure 10A) and limited operability can be seen for the AmAc system (can handle only ±2% feed ratio changes) as shown in Figure 10E. Table 4 also gives the dynamic performance for one-temperature/one-composition control for all five systems.

In summary, one temperature/one-composition control is recommended for the BuAc system, in which steady-state error can be eliminated without sacrificing closed-loop dynamics. For the AmAc system, limited operability is observed (Figure 10E) when the composition control is applied. For the MeAc system, the composition control leads to a large peak error and oscillatory response and thus a trade-off has to be made between the off-spec acetate composition and poor control performance. With respect to the EtAc and IPAc systems, the composition control provides little improvement in terms of the steady-state error.

Conclusion

The dynamics and control for three different types of reactive distillation flowsheets (types I, II, and III) are explored. This covers acetic acid esterification with different alcohols ranging from C_1 (MeOH) to C_5 (AmOH). Simultaneous reaction and separation lead to strongly nonlinearity to all five systems studied. However, the degree of nonlinearity can be analyzed qualitatively or computed quantitatively. The results indicate that the steady-state gains "sign reversal" and input multiplicity are unavoidable for all five of these reactive distillation systems. A systematic design procedure is proposed to devise the control structures for all three types of flowsheets. The simulation results reveal that workable temperature control can be obtained for these highly nonlinear processes with simple control. Moreover, the closed-loop systems do behave as the preliminary nonlinear analyses predict and inherent strong nonlinearity does lead to asymmetrical responses, especially for the MeAc and AmAc systems. Because of steady-state offsets in the product composition, a one-temperature/one-composition control structure is proposed to maintain on-aim product quality. This offers an alternative when the temperature control shows medium to large offsets in product composition. With respect to flowsheets, the type II flowsheet

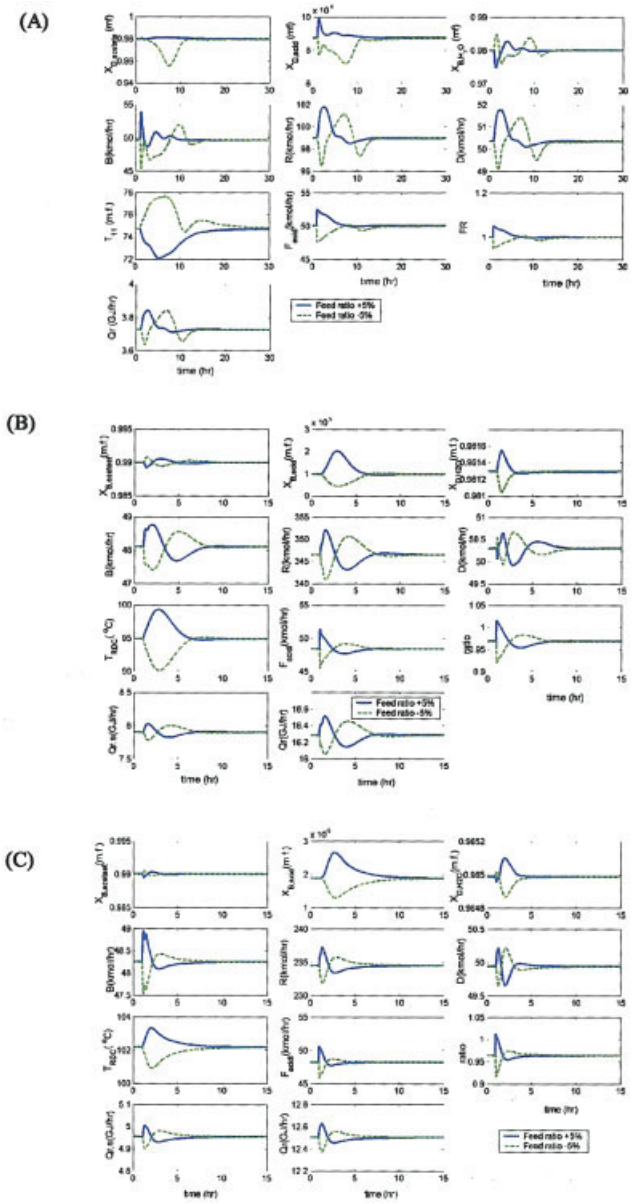

Figure 10. Composition control responses for ±5% feed ratio changes for (A) MeAc, (B) EtAc, (C) IPAc, and (D) BuAc, and ±2% changes for (E) AmAc systems.

[Color figure can be viewed in the online issue, which is available at www.interscience.wiley.com.]

(EtAc and IPAc) is divided into two units separated by a large decanter. This somewhat damps out the disturbance between the RDC and the stripper, which subsequently leads to a more controllable process. The flowsheet (BuAc and AmAc) where a decanter is used provides a natural one-end composition control by liquid–liquid equilibrium. Interaction between top and bottom composition control can thus be alleviated. Finally, the type I flowsheet cannot avoid either the inherent nonlinearity or the dynamic interactions. The nonlinearity and strong interactions lead to a very difficult process to control.

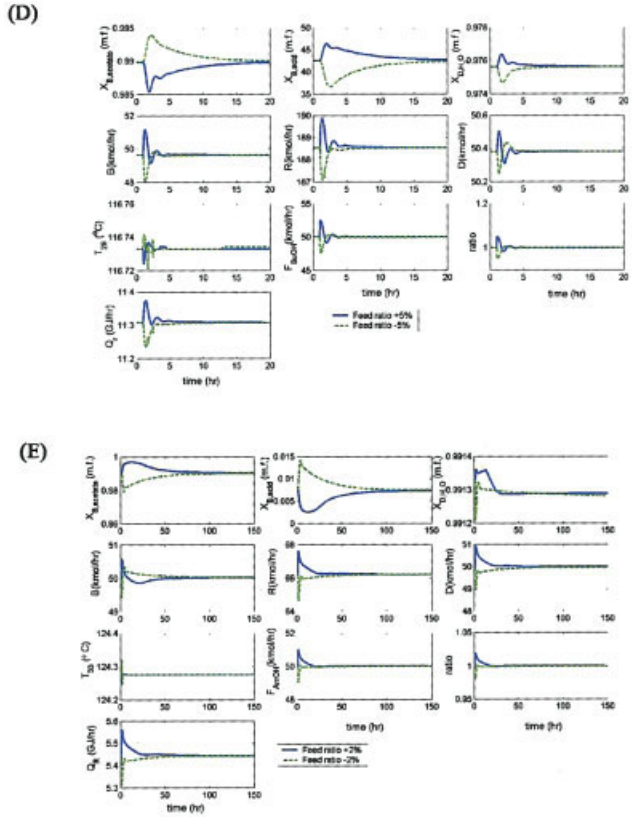

Figure 10. Continued.

Acknowledgments

We are grateful for the thoughtful and critical comments made by the reviewers, resulting in a much improved paper. We also thank Schweickhardt and Allgower providing us internal materials for nonlinear analysis. This work was supported by the Ministry of Economic Affairs under Grant 92-EC-17-A-09-S1-019.

Notation

AmAc = amyl acetate
AmOH = amyl alcohol (*n*-pentanol)
B = bottom flow rate (Type II: stripper)
BuAc = *n*-butyl acetate
BuOH = *n*-butanol
D = distillate flow rate (Type II: aqueous phase flow rate)
EtAc = ethyl acetate
EtOH = ethanol
F_{Acid} = acid feed flow rate
F_{Alcohol} = alcohol feed flow rate
FR = feed ratio
IPAc = isopropyl acetate
IPOH = isopropanol
K_c = controller gain
MeAc = methyl acetate
MeOH = methanol
mf = mole fraction
NF_{Acid} = acid feed location
NF_{Alcohol} = alcohol feed location
N_{R} = number of trays in the rectifying section
NRG = nonsquare relative gain
N_{rxn} = number of trays in the reactive section
N_{S} = number of trays in the stripping section
N_{T} = total number of trays
Q_{C} = condenser duty
Q_{R} = reboiler duty of the reactive distillation column
$Q_{\mathrm{R},S}$ = reboiler duty of the stripper

R = reflux flow rate
RDC = reactive distillation column
RGA = relative gain array
T_j = temperature on tray j
TAC = total annual cost
X_B = liquid mole fraction in the bottom product
X_D = liquid mole fraction in the distillate

Literature Cited

1. Malone MF, Doherty MF. Reactive distillation. *Ind Eng Chem Res.* 2000;39:3953.
2. Doherty MF, Malone MF. *Conceptual Design of Distillation System*. New York, NY: McGraw-Hill; 2001.
3. Sundmacher K, Kienle A. *Reactive Distillation: Status and Future Directions*. Weinheim, Germany: Wiley-VCH; 2003.
4. Taylor R, Krishna R. Modelling reactive distillation. *Chem Eng Sci.* 2000;55:5183-5229.
5. Roat S, Downs J, Vogel E, Doss J. Integration of rigorous dynamic modeling and control system synthesis for distillation columns. In *Chemical Process Control—CPC III*. Amsterdam, The Netherlands: Elsevier; 1986:99-138.
6. Luyben WL. *Practical Distillation Control*. New York, NY: Van Nostrand Reinhold; 1992.
7. Al-Arfaj MA, Luyben WL. Comparison of alternative control structures for an ideal two-product reactive distillation column. *Ind Eng Chem Res.* 2000;39:3298-3307.
8. Al-Arfaj MA, Luyben WL. Comparative control study of ideal and methyl acetate reactive distillation. *Chem Eng Sci.* 2002;57:5039-5050.
9. Kaymak DB, Luyben WL. Quantitative comparison of reactive distillation with conventional multiunit reactor/column/recycle systems for different chemical equilibrium constants. *Ind Eng Chem Res.* 2004;43:2493-2507.
10. Kaymak DB, Luyben WL. Comparison of two types of two-temperature control structures for reactive distillation columns. *Ind Eng Chem Res.* 2005;44:4625-4640.
11. Sneesby MG, Tade MO, Smith TN. Two-point control of a reactive distillation column for composition and conversion. *J Process Control.* 1999;9:19-31.
12. Engell S, Fernholz G. Control of a reactive separation process. *Chem Eng Process.* 2003;42:201-210.
13. Grüner S, Mohl KD, Kienle A, Gilles ED, Fernholz G, Fredrich M. Nonlinear control of a reactive distillation column. *Control Eng Pract.* 2003;11:915-925.
14. Tang YT, Hung SB, Chen YW, Huang HP, Lee MJ, Yu CC. Design of reactive distillations for acetic acid esterification with different alcohols. *AIChE J.* 2005;51:1683-1699.
15. Luyben WL. Economic and dynamic impact of the use of excess reactant in reactive distillation systems. *Ind Eng Chem Res.* 2000;39:2935-2946.
16. Huang SG, Kuo CL, Hung SB, Chen YW, Yu CC. Temperature control of heterogeneous reactive distillation. *AIChE J.* 2004;50:2203-2216.
17. Chiang SF, Kuo CL, Yu CC, David SHW. Design alternatives for the amyl acetate process: Coupled reactor/column and reactive distillation. *Ind Eng Chem Res.* 2002;41:3233-4246.
18. Menold PH, Allgöwer F, Pearson RK. Nonlinear structure identification of chemical processes. *Comput Chem Eng.* 1997;21:S137-S142.
19. Hernjak N, Doyle FJ III. Correlation of process nonlinearity with closed-loop disturbance rejection. *Ind Eng Chem Res.* 2003;42:4611-4619.
20. Schweickhardt T, Allgower F. Quantitative nonlinearity assessment: An introduction to nonlinearity measure. In Seferlis P, Georgiadis MC, eds. *Integration of Process Design and Control*. Amsterdam, The Netherlands: Elsevier; 2004.
21. Schweickhardt T, Allgower F. *Linear Modeling Error and Steady-state Behaviour of Nonlinear Dynamical Systems*. Internal Report. Stuttgart, Germany: Institute of System Theory in Engineering, University of Stuttgart; 2005.
22. Chang JW, Yu CC. The relative gain for non-square multivariable systems. *Chem Eng Sci.* 1990;45:1309.
23. Shen SH, Yu CC. Use of relay-feedback test for automatic tuning of multivariable systems. *AIChE J.* 1994;40:627-646.
24. Bristol EH. On a new measure of interaction for multivariable process control. *IEEE Trans Autom Control.* 1966;AC11:133.

Manuscript received May 15, 2005, and revision received Oct. 23, 2005.